Plasma amyloid-beta ratios in autosomal dominant Alzheimer's disease: the influence of genotype

Antoinette O'Connor, MRCPI[1,2*], Josef Pannee, PhD[3,4*], Teresa Poole, MSc[1,5*], Charles Arber, PhD[6], Erik Portelius, PhD[3,4],Imogen J Swift, MSc[2], Amanda J Heslegrave, PhD[2], Emily Abel, MSc[2], Nanet Willumsen, PhD[6], Helen Rice, MSc[1,2], Philip SJ Weston, PhD[1], Natalie S Ryan, PhD[1,2], James M Polke PhD[7], Jennifer M Nicholas PhD[1,5], Simon Mead PhD[8,9], Selina Wray PhD[6], Lucía Chávez-Gutiérrez PhD[10,11], Chris Frost MA DipStat (Cantab)[5],Kaj Blennow, MD, PhD[3,4], Henrik Zetterberg, MD, PhD[2,3,4 #] and Nick C Fox, FMedSci[1,2#]

***/[#]These authors contributed equally to this work.**

Abstract

In-vitro studies of autosomal dominant Alzheimer's disease implicate longer amyloid-beta peptides in disease pathogenesis, however less is known about the behaviour of these mutations *in-vivo*. In this cross-sectional cohort study, we used liquid chromatography-tandem mass spectrometry to analyse 66 plasma samples from individuals who were at-risk of inheriting a mutation or were symptomatic. We tested for differences in amyloid-beta42:38, 42:40 and 38:40 ratios between *presenilin1* and *amyloid precursor protein* carriers. We examined the relationship between plasma and *in-vitro* models of amyloid-beta processing and tested for associations with parental age at onset. 39 participants were mutation carriers (28 *presenilin1* and 11 *amyloid precursor protein).* Age- and sex-adjusted models showed marked differences in plasma amyloid-beta between genotypes: higher amyloid-beta42:38 in *presenilin1* versus *amyloid precursor protein* ($p<0.001$) and non-carriers ($p<0.001$); higher amyloid-beta38:40 in *amyloid precursor protein* versus *presenilin1* ($p<0.001$) and non-carriers ($p<0.001$); while amyloid-beta42:40 was higher in both mutation groups compared to non-carriers (both $p<0.001$). Amyloid-beta profiles were reasonably consistent in plasma and cell lines. Within

presenilin1, models demonstrated associations between amyloid-beta42:38, 42:40 and 38:40 ratios and parental age at onset. *In-vivo* differences in amyloid-beta processing between *presenilin1* and *amyloid precursor protein* carriers provide insights into disease pathophysiology, which can inform therapy development.

Author affiliations:

(1) Dementia Research Centre, UCL Queen Square Institute of Neurology, London, WC1N 3BG, United Kingdom

(2) UK Dementia Research Institute at UCL, London, WC1E 6AU, United Kingdom

(3) Department of Psychiatry and Neurochemistry, Institute of Neuroscience and Physiology, Sahlgrenska Academy at University of Gothenburg, S-431 80 Mölndal, Sweden

(4) Clinical Neurochemistry Laboratory, Sahlgrenska University Hospital, S-431 80 Mölndal, Sweden

(5) Department of Medical Statistics, London School of Hygiene & Tropical Medicine, London, WC1E 7HT, United Kingdom

(6) Department of Neurodegenerative Disease, UCL Queen Square Institute of Neurology, London, WC1N 3BG, UK

(7) Neurogenetics Laboratory, National Hospital for Neurology and Neurosurgery, University College London Hospitals NHS Foundation Trust, London WC1N 3BG, UK

(8) National Prion Clinic, National Hospital for Neurology and Neurosurgery, University College London Hospitals NHS Foundation Trust, London WC1N 3BG, UK

(9) MRC Prion Unit at UCL, UCL Institute of Prion Diseases, 33 Cleveland Street, London W1W 7FF, UK

(10) VIB-KU Leuven Center for Brain & Disease Research, 3000 Leuven, Belgium

(11) Department of Neurosciences, Leuven Research Institute for Neuroscience and Disease (LIND), KU Leuven,3000 Leuven, Belgium

Corresponding author: Professor Nick C Fox, email: n.fox@ucl.ac.uk, telephone: +44 (0)20 3448 477, address: First floor, 8-11 Queen Square, London, WC1N 3AR

Running title: Plasma amyloid in Alzheimer's disease

Keywords: autosomal dominant Alzheimer's disease; blood biomarkers; dementia; amyloid-beta

Abbreviations: Age at onset = AAO; Amyloid-beta = Aβ; Amyloid precursor protein = APP; Autosomal dominant Alzheimer's disease = ADAD; Clinical dementia rating scale = CDR; Estimated years to symptom onset = EYO; induced pluripotent stem cell = iPSC; Presenilin1 = *PSEN1;* Presenilin2 = *PSEN2*

Introduction

Understanding Alzheimer's disease pathogenesis is critical to realising disease-modifying treatments. Autosomal dominant Alzheimer's disease (ADAD), caused by mutations in presenilin 1/2 *(PSEN1/2)* or amyloid precursor protein (*APP)*, is a valuable model for characterising the molecular drivers of Alzheimer's disease.[1]

PSEN1, the catalytic subunit of γ-secretase, sequentially cuts APP: initial endopeptidase cleavage generates an amyloid-beta (Aβ) peptide, either Aβ49 (major product) or Aβ48 (minor product).[2] Subsequent proteolysis largely occurs down two pathways: Aβ49>46>43>40 or Aβ48>45>42>38.[3] As Aβ49 is the predominant endopeptidase cleavage product, normal APP processing largely leads to Aβ40 formation.[2] Pathogenic ADAD mutations alter APP processing resulting in more, and/or longer, aggregation prone, Aβ peptides, which accelerate cerebral amyloid accumulation leading to typical symptom onset in 30s to 50s.[4,5]

Both *APP* and *PSEN1/2* mutations increase production of longer (e.g. Aβ42) relative to shorter (e.g. Aβ40) peptides.[5] However, there are intriguing inter-mutation differences in Aβ profiles. *PSEN1* mutant lines produce increased Aβ42:38 ratios reflecting impaired γ-secretase processivity.[5,6] In contrast, *APP* mutations at the γ-secretase cleavage site increase Aβ38:40 ratios, consistent with preferential processing down the Aβ48 pathway.[6] To date, studies examining the influence of ADAD genotypes on Aβ ratios *in-vivo* have been lacking.

Increasingly sensitive mass spectrometry-based assays now make it possible to measure concentrations of different Aβ moieties in plasma.[7] Therefore, we aimed to analyse plasma Aβ levels in an ADAD cohort, explore influences of genotype and clinical stage, and examine relationships between ratios and both parental age at onset (AAO) and estimated years to/from symptom onset (EYO), while also assessing consistency with *in-vitro* models of Aβ processing.

Materials and methods

Study design and participants

We recruited 66 participants from UCL's longitudinal ADAD study; details described previously.[1] Samples were collected from August 2012 to July 2019 and concomitantly a semi-structured health questionnaire and clinical dementia rating (CDR) scale were completed.[8] EYO was calculated by subtracting parental AAO from the participant's age. Participants were defined as symptomatic if global CDR was >0. ADAD mutation status, determined using Sanger sequencing, was provided only to statisticians, ensuring blinding of participants and clinicians. The study had local Research Ethics Committee approval; written informed consent was obtained from all participants or a consultee.

Measurement of plasma Aβ levels

EDTA plasma samples were processed, aliquoted, and frozen at −80°C according to standardised procedures and shipped frozen to the Clinical Neurochemistry Laboratory, Sahlgrenska University Hospital, for analysis blinded to participants' mutation status and diagnosis. Samples were analysed using a liquid chromatography-tandem mass spectrometry

method using an optimized protocol for immunoprecipitation for improved analytical sensitivity (Appendix 1, Supplementary Fig. 1, Supplementary Fig 2).[9] Pooled plasma samples were used to track assay performance; intra- and inter-assay coefficients of variation were <5%.

Correlation of Aβ ratios in plasma and in induced pluripotent stem cell (iPSC) neurons

A sub-study investigated the consistency of Aβ profiles between plasma and iPSC-derived neurons. Aβ profiles were compared based on mutation for 8 iPSC-lines; data from 6 iPSC-lines previously reported by Arber *et al*.[6]. Mutations tested were *APP* V717I (n=2), *PSEN1* Intron 4 (n=1), Y115H (n=1), M139V (n=1), R278I (n=1) and E280G (n=2). Plasma and iPSC samples were from the same participant or, where matched plasma was unavailable, plasma from a carrier of the same mutation, and if possible a family member. Aβ42:40, Aβ38:40 and Aβ42:38 ratios were normalised by taking the ratio of the value for each mutation carrier to the control median for each experimental setting (n=27 non-carriers for plasma, n=5 iPSC controls lines from non-ADAD families) (ratio values Supplementary Table 1).

iPSC-neuronal Aβ was quantified as previously reported Arber *et al.*[6]. Briefly, iPSCs were differentiated to cortical neurons for 100 days and then 48 hour-conditioned culture supernatant was centrifuged removing cell debris. Aβ was analysed via electrochemiluminescence on the MSD V-Plex Aβ peptide panel (6E10), according to manufacturer's instructions.

Statistical analysis

Summary descriptive statistics were calculated by mutation type (*PSEN1*, *APP,* non-carriers) and box plots produced for Aβ42:38, Aβ38:40 and Aβ42:40 ratios. Box plots were presented by mutation type (*PSEN1* vs *APP* vs non-carriers), and then individually for *PSEN1* and *APP* carriers by clinical stage (presymptomatic vs symptomatic vs non-carriers) (Fig. 1). Aβ ratios are displayed on logarithmic scales. Age- and sex-adjusted differences were estimated between mutation type for each ratio; as were differences by clinical stage for each ratio, separately for *APP* and *PSEN1* carriers. These comparisons were made using mixed models including random intercepts for clusters comprising individuals from the same family and group, with random

intercept and residual variances allowed to differ for the groups being compared. Pairwise comparisons were only carried out if a joint test provided evidence of differences. Ratios were log-transformed; estimated coefficients were back-transformed to multiplicative effects.

The relationship between parental AAO, EYO and age (EYO = age – AAO) means that it is not possible to estimate separate effects of AAO and EYO on Aβ ratios adjusting for age using a conventional statistical analysis: if age is held constant then a one-year increase in AAO implies a one year decrease in EYO and vice versa, hence their effects are aliased. However the aim here should be to allow for 'normal ageing' (as observed in non-carriers), and this is possible. For each combination of mutation carrier group (*PSEN1* and *APP*) and Aβ ratio a separate mixed model was fitted jointly to the carrier group and the non-carrier group. Each model allowed the logarithm of the Aβ ratio to depend on AAO, EYO and sex (but not age) in the carrier group, and on just sex and age (estimating 'normal ageing') in the non-carrier group. Random effects were included as in the between group comparisons above. In the carrier group the effect of AAO adjusted for EYO, sex and (non-carrier) 'normal ageing' was obtained by subtracting the 'normal ageing' effect from the AAO effect (adjusted for sex and EYO). Analogously the effect of EYO adjusted for AAO, sex and 'normal ageing' was obtained by subtracting the 'normal ageing' effect from the EYO effect (adjusted for sex and AAO) in the carrier group. For Aβ42:38 in *PSEN1* carriers there was evidence also to include a quadratic term for parental AAO. For each analysis the estimated geometric mean ratio (and 95% confidence interval) was plotted against parental AAO, standardising to an equal mix of males/females, an EYO of 0 (i.e. the point of symptom onset), and adjusted for 'normal ageing' relative to age 43 (the average age of mutation carriers). Analogous plots of estimated geometric mean ratio (and 95% confidence interval) against EYO were standardised to an equal mix of males/females, an AAO of 43 (average age of mutation carriers), and adjusted for 'normal ageing' relative to age 43.

Spearman correlation coefficients were calculated to assess the association between plasma and iPSC-neuron Aβ ratios.

Analyses were performed using Stata v16.

Data availability

Data are available upon reasonable request from qualified investigators, adhering to ethical guidelines.

Results

Demographic and clinical characteristics are presented in Table 1: 27 non-carriers; 39 mutation carriers (28 *PSEN1*, 11 *APP*); Supplementary Table 2 gives mutation details.

Age- and sex-adjusted models showed marked differences in plasma Aβ between *PSEN1* and *APP* carriers. The geometric mean of Aβ42:38 was higher in *PSEN1* compared to both *APP* carriers (69% higher, 95%*CI:* 39%, 106%; $p<0.001$) and non-carriers (64% higher, 95%*CI:* 36%, 98%; $p<0.001$), while there was no evidence of a difference between *APP* carriers and non-carriers ($p= 0.60$) (Fig. 1A).

Plasma Aβ42:40 was raised in both *PSEN1* and *APP*; compared to non-carriers the adjusted geometric mean was 31% higher (95%*CI:* 16%, 49%; $p<0.001$) in *PSEN1* and 61% higher (95%*CI:* 44%, 80%; $p<0.001$) in *APP* (Fig. 1D). There were also inter-mutation differences in Aβ42:40: the geometric mean was 22% higher (95%*CI:* 8%, 38%; $p=0.001$) in *APP* compared to *PSEN1* carriers.

The geometric mean of Aβ38:40 was higher in *APP* carriers compared to both *PSEN1* carriers (101% higher, 95%*CI:* 72%, 135 %; $p<0.001$) and non-carriers (61% higher, 95%*CI:* 41%, 84%; $p<0.001$) (Fig. 1G). While in *PSEN1,* Aβ38:40 was reduced compared to non-carriers (geometric mean 20% lower, 95%*CI*: 10%, 29%, $p<0.001$).

For Aβ42:40 ratios, group differences remained significant when separately comparing non-carriers to (i) presymptomatic (18% higher, 95%*CI:* 3%, 36%, $p=0.02$) and symptomatic (47% higher, 95% *CI:* 23%, 76%, $p<0.001$) *PSEN1* carriers, and to (ii) presymptomatic (62% higher,

95% *CI:* 44%, 82%, $p<0.001$) and symptomatic (62% higher, 95% *CI:* 37%, 92%, $p<0.001$) *APP* carriers (Figs. 1E, 1F). Within *PSEN1,* the geometric mean of Aβ42:40 was also 24% higher (95%*CI:* 2%, 52%; $p=0.03$) in symptomatic compared to presymptomatic carriers (Fig. 1E). There were no statistically significant differences between presymptomatic and symptomatic *PSEN1* carriers in Aβ42:38 ($p=0.11$; Fig 1B) or Aβ38:40 ($p=0.54$; Fig. 1H). Additionally, no significant differences were observed in the Aβ42:40, Aβ42:38 or Aβ38:40 ratios between presymptomatic and symptomatic *APP* carriers (all *p*-values>0.50) (Fig. 1C, 1F, 1I).

Using models that adjusted for sex, EYO and 'normal ageing', we found significant associations between all three ratios and parental AAO in *PSEN1* carriers (all *p*-values <0.03) (Fig. 2). Higher Aβ42:38 and Aβ42:40 ratios were associated with earlier parental onset, while higher Aβ38:40 was associated with a later disease onset. For Aβ42:38 we included a quadratic term ($p=0.003$), which resulted in the estimated rate of change of Aβ42:38 reducing as parental AAO increased; a one-year increase in parental AAO was associated with a 9.4% decrease (95% *CI:* 5.3%,13.3%; $p<0.001$) in the geometric mean of Aβ42:38 at age 35 compared to a 4.4% decrease (95% *CI:* 2.9%, 5.9%; $p<0.001$) in the same measure at age 45. For both Aβ42:40 and Aβ38:40, the association with parental AAO was estimated to be constant across the age range investigated, a one-year increase in parental AAO was associated with a 1.6% decrease (95% *CI*: 0.2%, 3.1%; $p=0.03$) in Aβ42:40 and a 1.7% increase (95% *CI*: 0.4%, 3.0%; $p=0.008$) in the Aβ38:40. In *APP* carriers, there were no significant associations between Aβ42:40, Aβ42:38 or Aβ38:40 and parental AAO (all *p*-values ≥0.18; Supplementary Fig. 3).

In *PSEN1* and *APP* carriers, models that adjusted for sex, parental AAO and 'normal ageing' did not find any significant association between either Aβ42:40, Aβ42:38 or Aβ38:40 and EYO (Supplementary Figs. 4,5) ($p\geq0.06$). However, in *APP* carriers there was weak evidence of an association between Aβ42:40 and EYO: a one-year increase in EYO was associated with a 0.8% decrease (95% *CI*: 1.6% decrease, 0.0% increase, $p=0.06$) in the geometric mean of Aβ42:40.

Aβ ratios in plasma and iPSC-conditioned media were highly associated for both Aβ42:40 (*rho*=0.86, *p*=0.01) and Aβ38:40 (*rho*=0.79, *p*=.02), somewhat less so for Aβ42:38 (*rho*=0.61, *p*=0.10) (Fig. 3). While we did not observe perfect agreement in the Aβ42:38 ratio between plasma and iPSC lines (shown by solid line, Fig. 3), the direction of change in this ratio, i.e. either increased or decreased when compared to controls, was largely consistent across media.

Discussion

In this study we found increases in plasma Aβ42:40 in both *APP* and *PSEN1* carriers compared to non-carriers and marked differences in Aβ ratios between genotypes: Aβ42:38 was higher in *PSEN1* vs. *APP*, Aβ38:40 was higher in *APP* vs. *PSEN1*. Importantly, more aggressive *PSEN1* mutations (those with earlier ages of onset) had higher Aβ42:40 and Aβ42:38 ratios – *in-vivo* evidence of the pathogenicity of these peptide ratios.

These results offer insights into the pathobiology of ADAD and differential effects of *APP/PSEN1* genotype. Increased Aβ42:38 in *PSEN1* may be attributed to reduced conversion of Aβ42 (substrate) to 38 (product) relative to non-carriers – in contrast *APP* carriers showed near identical Aβ42:38 ratios compared to non-carriers. Strikingly, increases in Aβ42 relative to shorter Aβ moieties (≤40) were associated with earlier disease onset in *PSEN1*. Importantly there were no associations between Aβ ratios and EYO in *PSEN1* carriers, suggesting these ratios represent molecular drivers of disease as opposed to being markers of disease stage. Our *in-vivo* results recapitulate cell-based findings of reduced efficiency of γ-secretase processivity in *PSEN1* [6,10,11]; inefficiency attributed to impaired enzyme-substrate stability causing premature release of longer Aβ peptides.[10]

Parental AAO is an indicator of disease severity, with a younger AAO implying a more deleterious mutation. In *PSEN1* Aβ42:38 (a read-out of the efficiency of the fourth γ-secretase cleavage) showed a deceleration in the rate of change as parental AAO increases. This further supports the central pathogenic role of γ-secretase processivity in ADAD, especially in younger onset, aggressive forms of *PSEN1*.

In *APP*, production of Aβ38 relative to Aβ40 was increased. This is consistent with a shift in the site of endopeptidase-cleavage causing increased generation of Aβ48; the precursor substrate in the Aβ38 production line. Our study included *APP* mutations located near the γ-secretase cleavage site. Previous cell-based work involving mutations around this site also demonstrated increased trafficking along the Aβ48 pathway.[5,6,11] In contrast, *APP* duplications or mutations near the beta-secretase site are associated with non-differential increases in Aβ production.[12]

Changes in Aβ38:40 were also seen in *PSEN1* carriers; levels were reduced compared to both *APP* carriers and non-carriers. Declines in Aβ38:40 may reflect mutation effects on endopeptidase cleavage and/or γ-secretase processivity; changes in both processes have been described in *in-vitro* studies of *PSEN1*.[6,13] Premature release of longer (>Aβ43) peptides may contribute to falls in Aβ38:40; both increasing Aβ length and pathogenic *PSEN1* mutations are associated with destabilisation of the enzyme-substrate complex.[10] It will be important for future research to investigate the exact molecular drivers of declines in Aβ38:40 in *PSEN1,* especially as lower levels were associated with earlier disease onset.

We also saw inter-stage differences in APP processing; Aβ42:40 was higher in symptomatic compared to presymptomatic *PSEN1* carriers. The reason for this is unclear and should be treated cautiously given small group sizes and the absence of inter-stage differences in Aβ42:40 amongst *APP* carriers. However, post-symptomatic increases in plasma Aβ42 have been reported in Down syndrome.[14] It is possible that downstream pathogenic consequences of ADAD, such as cerebral amyloid angiopathy, may interact with, and modify, plasma levels. Additionally, as Aβ is produced peripherally in organs, muscle and platelets, systemic factors may contribute to inter-stage differences.[15]

Our results support the hypothesis that ADAD mutations increase *in-vivo* production of longer Aβ peptides (Aβ≥42) relative to Aβ40. This is consistent with cell- and blood-based studies in ADAD.[11,16] Additionally, we showed plasma Aβ profiles were recapitulated in iPSC-media with consistent profiles for the same mutation. There is some evidence that Aβ42:40 ratios also increase in the CSF of mutation carriers far from onset, however CSF levels then fall

significantly during the two decades before symptom onset[17]; reductions are attributed to "trapping" of longer peptides within cerebral plaques.[18] In sporadic Alzheimer's disease CSF, as well as plasma, Aβ42:40 levels also fall as cerebral amyloid plaques start to accumulate, with ratio levels remaining low thereafter.[19] In contrast, we show that plasma Aβ42:40 in both *APP* and *PSEN1* carriers was raised and did not fall below non-carriers levels, either before or after symptom onset. Taken together, these findings suggest that plasma Aβ ratios in ADAD are less susceptible to the effects of sequestration.

Study limitations include the small sample size, due to the rarity of ADAD, however we included a reasonably wide array of mutations. Secondly, ages at onset were estimated from parental AAO, while this offers a reasonable estimate there is variability within families and imprecision in determining AAO in a preceding, often deceased, generation.[20] Finally, future studies should measure Aβ moieties longer than Aβ42, and also investigate interactions between central and peripheral Aβ production (we lacked paired CSF).

In conclusion, we demonstrate the impact of pathogenic ADAD mutation on APP processing *in-vivo*. We show marked inter-mutation difference in Aβ profiles, with relative increases in longer peptides being associated with earlier disease onset. Our findings suggest that plasma Aβ ratios in ADAD may be useful biomarkers of APP processing. This is especially important as we enter an era of gene silencing therapies, and personalised medicine, where direct read-outs of gene function will be particularly valuable.

Funding

AOC is supported by an Alzheimer's Society clinical research training fellowship (AS-CTF-18-001), and acknowledges previous support from the Rosetrees Trust. CA is supported by a fellowship from the Alzheimer's Society (AS-JF-18-008) and SW is supported by an Alzheimer's Research UK Senior Research Fellowship (ARUK-SRF2016B-2). IS is supported by the UK Dementia Research Institute which receives its funding from DRI Ltd, funded by the UK Medical Research Council, Alzheimer's Society and Alzheimer's Research UK. PSJW

is supported by an MRC Clinical Research Training Fellowship. NSR is supported by a University of London Chadburn Academic Clinical Lectureship. HZ is a Wallenberg Scholar supported by grants from the Swedish Research Council (#2018-02532), the European Research Council (#681712), Swedish State Support for Clinical Research (#ALFGBG-720931) and the UK Dementia Research Institute at UCL. KB is supported by the Swedish Research Council (#2017-00915), the Alzheimer Drug Discovery Foundation (ADDF), USA (#RDAPB-201809-2016615), the Swedish Alzheimer Foundation (#AF-742881), Hjärnfonden, Sweden (#FO2017-0243), and European Union Joint Program for Neurodegenerative Disorders (JPND2019-466-236). CF, JMN and TP's academic collaboration with the Dementia Research Centre, UCL is supported by a grant to the DRC from Alzheimer's Research UK. NCF acknowledges support from Alzheimer's Research UK, the UK Dementia Research Institute and the NIHR UCLH Biomedical Research Centre. This work was supported by the NIHR UCLH/UCL Biomedical Research Centre, the Rosetrees Trust, the MRC Dementia Platform UK and the UK Dementia Research Institute at UCL which receives its funding from UK DRI Ltd, funded by the UK Medical Research Council, Alzheimer's Society and Alzheimer's Research UK, and the Swedish state under the agreement between the Swedish government and the County Councils, the ALF-agreement (#ALFGBG-715986). Professor Nick Fox had full access to all the data in the study and takes responsibility for the integrity of the data and the accuracy of the data analysis.

Competing interests

KB has served as a consultant, at advisory boards, or at data monitoring committees for Abcam, Axon, Biogen, JOMDD/Shimadzu. Julius Clinical, Lilly, MagQu, Novartis, Roche Diagnostics, and Siemens Healthineers, and is a co-founder of Brain Biomarker Solutions in Gothenburg AB (BBS), which is a part of the GU Ventures Incubator Program. HZ has served at scientific advisory boards for Denali, Roche Diagnostics, Wave, Samumed and CogRx, has given lectures in symposia sponsored by Fujirebio, Alzecure and Biogen, and is a co-founder of Brain Biomarker Solutions in Gothenburg AB, a GU Ventures-based platform company at the University of Gothenburg. NCF reports consultancy for Roche, Biogen and Ionis, and serving on a Data Safety Monitoring Board for Biogen. HR has undertaken consultancy for Roche.

References

1. Ryan NS, Nicholas JM, Weston PSJ, et al. Clinical phenotype and genetic associations in autosomal dominant familial Alzheimer's disease: a case series. *Lancet Neurol*. 2016;15(13):1326-1335. doi:10.1016/S1474-4422(16)30193-4
2. Sato T, Dohmae N, Qi Y, et al. Potential Link between Amyloid β-Protein 42 and C-terminal Fragment γ 49-99 of β-Amyloid Precursor Protein. *J Biol Chem*. 2003;278(27):24294-20301. doi:10.1074/jbc.M211161200
3. Takami M, Nagashima Y, Sano Y, et al. γ-Secretase: Successive tripeptide and tetrapeptide release from the transmembrane domain of β-carboxyl terminal fragment. *J Neurosci*. 2009;29(41):13042-13052. doi:10.1523/JNEUROSCI.2362-09.2009
4. Bateman RJ, Xiong C, Benzinger TLLS, et al. Clinical and Biomarker Changes in Dominantly Inherited Alzheimer's Disease. *N Engl J Med*. 2012;367(9):795-804. doi:10.1056/NEJMoa1202753
5. Chávez-Gutiérrez L, Bammens L, Benilova I, et al. The mechanism of γ-Secretase dysfunction in familial Alzheimer disease. *EMBO J*. 2012;31(10):2261-2274. doi:10.1038/emboj.2012.79
6. Arber C, Toombs J, Lovejoy CC, et al. Familial Alzheimer's disease patient-derived neurons reveal distinct mutation-specific effects on amyloid beta. *Mol Psychiatry*. Published online April 12, 2019:1. doi:10.1038/s41380-019-0410-8
7. Schindler SE, Bollinger JG, Ovod V, et al. High-precision plasma β-amyloid 42/40 predicts current and future brain amyloidosis. *Neurology*. 2019;93(17):e1647-e1659. doi:10.1212/WNL.0000000000008081
8. Morris JC. The Clinical Dementia Rating (CDR): Current version and scoring rules. *Neurology*. 1993;43(11):2412-2412. doi:10.1212/WNL.43.11.2412-a
9. Pannee J, Törnqvist U, Westerlund A, et al. The amyloid-β degradation pattern in plasma--a possible tool for clinical trials in Alzheimer's disease. *Neurosci Lett*. 2014;573:7-12. doi:10.1016/j.neulet.2014.04.041

10. Szaruga M, Munteanu B, Lismont S, et al. Alzheimer's-Causing Mutations Shift Aβ Length by Destabilizing γ-Secretase-Aβn Interactions. *Cell*. 2017;170(3):443-456.e14. doi:10.1016/J.CELL.2017.07.004
11. Szaruga M, Veugelen S, Benurwar M, et al. Qualitative changes in human γ-secretase underlie familial Alzheimer's disease. *J Exp Med*. 2015;212(12):2003-2013. doi:10.1084/jem.20150892
12. Hunter S, Brayne C. *Understanding the Roles of Mutations in the Amyloid Precursor Protein in Alzheimer Disease*. Vol 23. Nature Publishing Group; 2018:81-93. doi:10.1038/mp.2017.218
13. Fernandez MA, Klutkowski JA, Freret T, Wolfe MS. Alzheimer presenilin-1 mutations dramatically reduce trimming of long amyloid β-peptides (Aβ) by γ-secretase to increase 42-to-40-residue Aβ. *J Biol Chem*. 2014;289(45):31043-31052. doi:10.1074/jbc.M114.581165
14. Fortea J, Vilaplana E, Carmona-Iragui M, et al. Clinical and biomarker changes of Alzheimer's disease in adults with Down syndrome: a cross-sectional study. *Lancet*. 2020;395(10242):1988-1997. doi:10.1016/S0140-6736(20)30689-9
15. Wang J, Gu BJ, Masters CL, Wang Y-J. A systemic view of Alzheimer disease — insights from amyloid-β metabolism beyond the brain. *Nat Rev Neurol*. 2017;13(10):612-623. doi:10.1038/nrneurol.2017.111
16. Reiman EM, Quiroz YT, Fleisher AS, et al. Brain imaging and fluid biomarker analysis in young adults at genetic risk for autosomal dominant Alzheimer's disease in the presenilin 1 E280A kindred: a case-control study. *Lancet Neurol*. 2012;11(12):1048-1056. doi:10.1016/S1474-4422(12)70228-4
17. Schindler SE, Li Y, Todd KW, et al. Emerging cerebrospinal fluid biomarkers in autosomal dominant Alzheimer's disease. *Alzheimer's Dement*. 2019;15(5):655-665. doi:10.1016/J.JALZ.2018.12.019
18. Potter R, Patterson BW, Elbert DL, et al. Increased in vivo amyloid-b42 production, exchange, and loss in presenilin mutation carriers. *Sci Transl Med*. 2013;5(189):189ra77-189ra77. doi:10.1126/scitranslmed.3005615
19. Palmqvist S, Insel PS, Stomrud E, et al. Cerebrospinal fluid and plasma biomarker trajectories with increasing amyloid deposition in Alzheimer's disease. *EMBO*

Mol Med. 2019;11(12):e11170. doi:10.15252/emmm.201911170

20. Pavisic IM, Nicholas JM, O'Connor A, et al. Disease duration in autosomal dominant familial Alzheimer disease. *Neurol Genet*. 2020;6(5):e507. doi:10.1212/NXG.0000000000000507

Figures

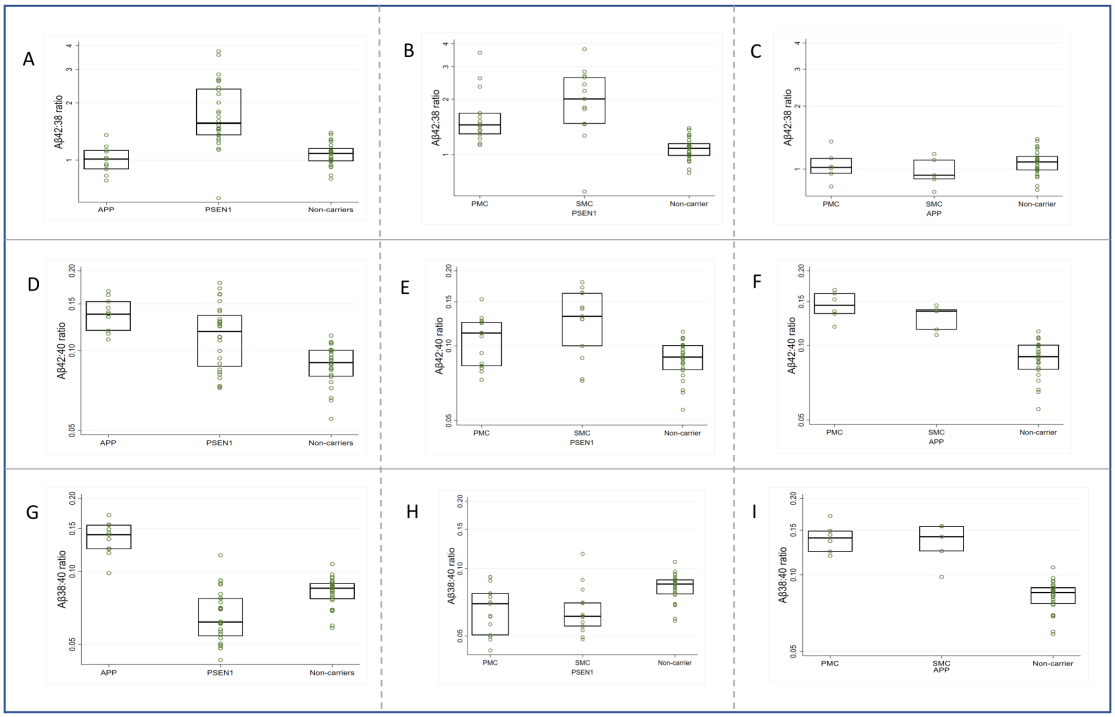

Figure 1: Box plots for observed plasma Aβ ratios. Plasma (**1A-C**) Aβ42:38, (**1D-F)** Aβ42:40 and **(1G-I)** Aβ38:40 ratios are shown with the y-axis on a logarithmic scale. Mutation carriers were divided into (**1A, 1D, 1G**) *APP* and *PSEN1* carriers and non-carriers; (**1B, 1E, 1H)** *PSEN1* presymptomatic and symptomatic mutation carriers and non-carriers and (**1C, 1F,**

1I) *APP* presymptomatic and symptomatic mutation carriers and non-carriers. Boxes show the median and first and third quartiles. Dots represent individual observations.

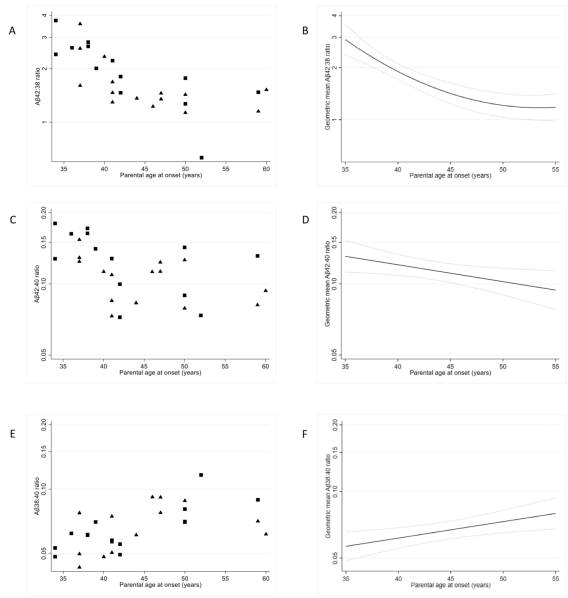

Figure 2: Plasma Aβ ratios against parental AAO in *PSEN1* carriers.

Scatter plots of observed plasma **(A)** Aβ42:38 **(C)** Aβ42:40 and **(E)** Aβ38:40 values against parental age at onset (AAO). Symptomatic mutation carriers are identified by square symbols and presymptomatic mutation carriers by triangle symbols.

Modelled geometric mean of plasma **(B)** Aβ42:38 **(D)** Aβ42:40 and **(F)** Aβ38:40 against parental AAO in *PSEN1* carriers; models adjust for EYO, sex and 'normal ageing' in non-carriers. The trajectories displayed contain an equal mix of males/females and are adjusted for 'normal ageing' relative to age 43 (the average age of mutation carriers). EYO is set at 0, i.e. point of symptom onset, in all three trajectory plots.

The y-axis scale is logarithmic in all panes.

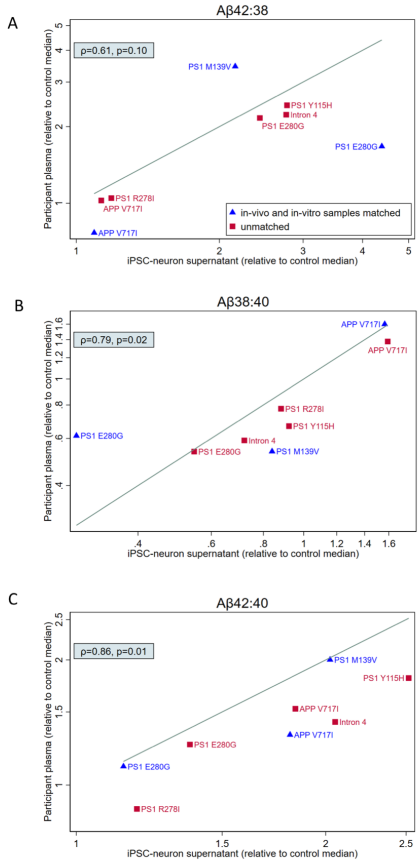

Figure 3: Comparison of Aβ processing *in-vivo* and *in-vitro*. Scatterplot comparing Aβ ratios profiles in plasma and iPSC derived neurons for eight mutation carriers. One to one comparison of Aβ ratios normalised to the median of controls for each experimental setting (n=27 non-carrier controls for plasma, n=5 iPSC lines from controls who were not members of ADAD families); values >1 indicate higher ratio in mutation carrier compared to median of controls whereas values <1 indicate lower ratio in mutation carrier compared to median of controls. Matched samples (plasma and iPSC samples donated by the same donor) are identified with triangle symbols. Unmatched samples (plasma and iPSC samples donated by different participants who carry the same mutation, and where possible are members of the same family) are identified by square symbols. The y-axis scale is logarithmic in all panes. Spearman's rho and the associated p-value are shown for each scatter plot. The line displayed on each

scatterplot represents line of perfect agreement i.e. x=y.

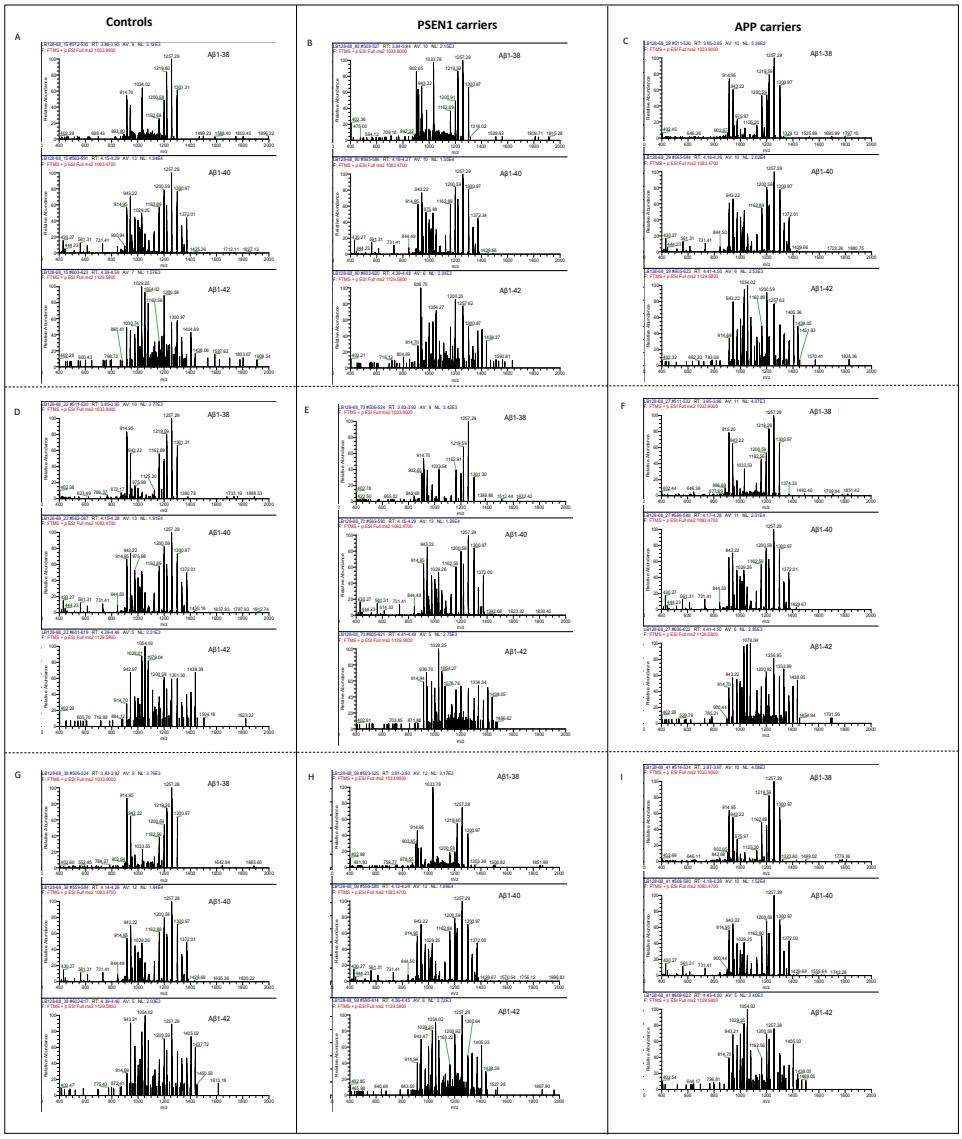

Figure 1: Representative mass spectrometry (MS) spectra for Aβ38, Aβ40 and Aβ42.
Representative MS profiles for 3 non-carrier controls **(1A, 1D, 1G**), 3 *PSEN1* carriers (**1B, 1E, 1H)** and *APP* carriers (**1C, 1F, 1I**). Panes **1B** and **1C** display profiles of presymptomatic mutation carriers, while panes **1E, 1F,1H, 1I** display profiles of symptomatic mutation carriers.

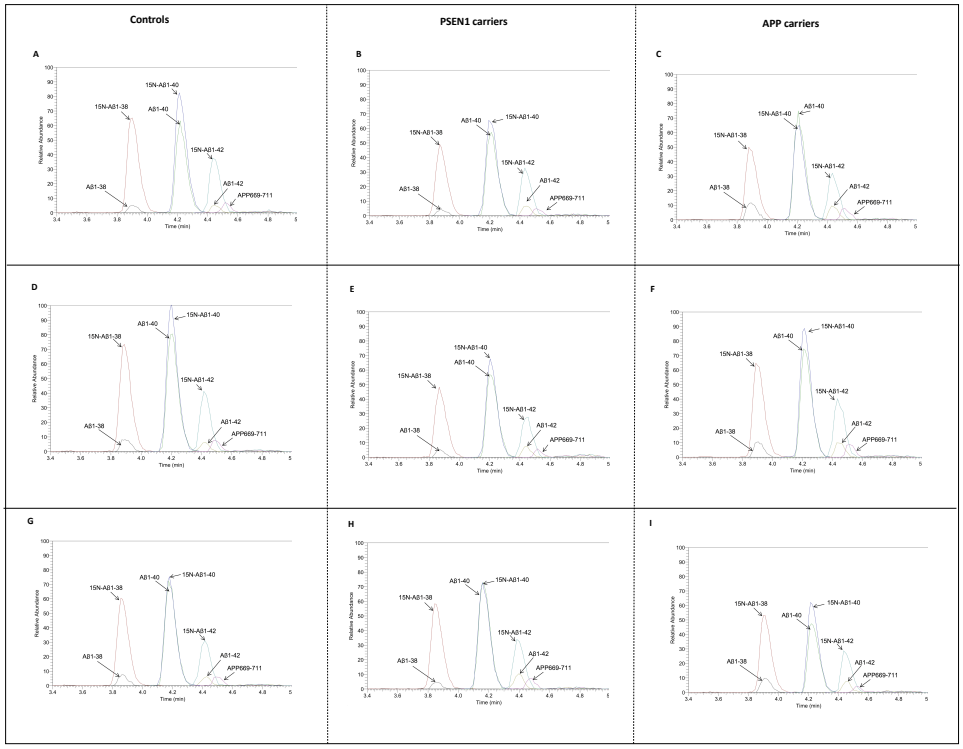

Supplementary figure 2: Representative chromatograms of the detected peptides and their corresponding internal standards
Representative chromatograms for 3 non-carrier controls (**1A, 1D, 1G**), 3 *PSEN1* carriers (**1B, 1E, 1H)** and *APP* carriers (**1C, 1F, 1I**). Panes **1B** and **1C** display profiles of presymptomatic mutation carriers, while panes **1E, 1F,1H, 1I** display profiles of symptomatic mutation carriers.

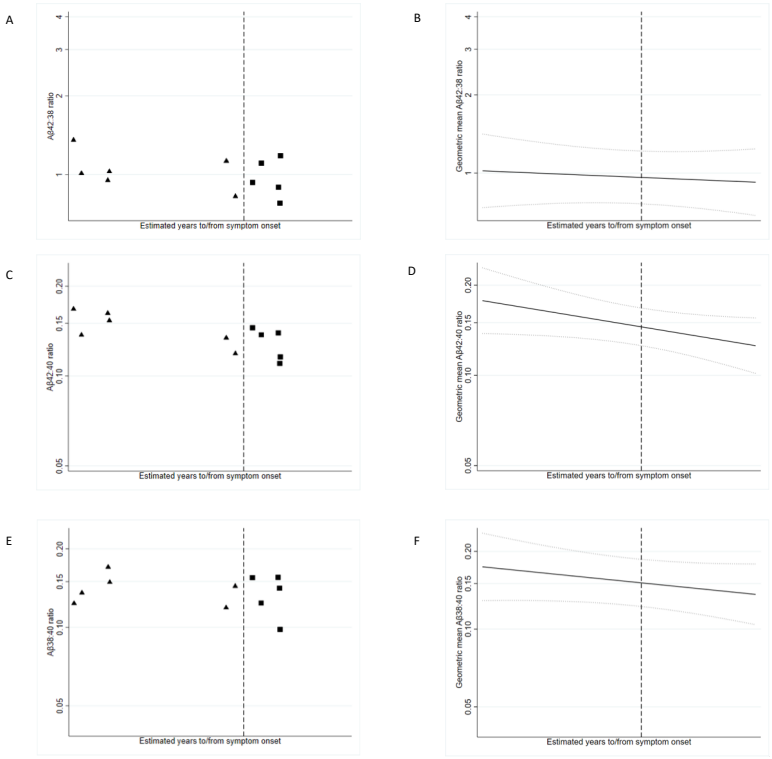

Supplementary figure 5: Plasma Aβ ratios against estimated years to/from symptom onset (EYO) in *APP* carriers.

Scatter plots of observed plasma **(A)** Aβ42:38 **(C)** Aβ42:40 and **(E)** Aβ38:40 values against EYO. All scatter plots show values for *APP* carriers only. Symptomatic mutation carriers are identified by square symbols and presymptomatic mutation carriers by triangle symbols.
Modelled geometric mean of plasma **(B)** Aβ42:38 **(D)** Aβ42:40 and **(F)** Aβ38:40 against EYO in *APP* carriers. The trajectories displayed contain an equal mix of males/females and are adjusted to 'normal ageing' in non-carriers relative to age 43 (average age of mutation carriers). Parental AAO is set at 43 in all three trajectory plots. Models, which adjusted for parental AAO, sex and 'normal ageing', did not show evidence of any significant associations between either Aβ42:38, Aβ42:40 or Aβ38:40 and EYO: for Aβ42:38 a one-year increase in EYO was associated with an estimated 0.2% decrease (95% CI: 1.2% decrease, 0.7% increase; p=0.63); for Aβ42:40 an estimated 0.8% decrease (95% CI: 1.6% decrease, 0.0% increase; p=0.06); for Aβ38:40 an estimated 0.6% decrease (95% CI:1.5% decrease, 0.3% increase; p=0.21). To maintain blinding of mutation status, the values of the x-axis for all EYO plots have been removed. The y-axis scale is logarithmic in all panes.

	iPSC 42:38	iPSC 42:40	iPSC 38:40	Plasma 42:38	Plasma 42:40	Plasma 38:40
Controls (median (IQR))	0.425 (0.418,0.429) (n=5)	0.110 (0.108,0.111) (n=5)	0.268 (0.258,0.270) (n=5)	1.083 (0.989, 1.154) (n=27)	0.090 (0.800, 0.100) (n=27)	0.085 (0.077, 0.089) (n=27)
APP V717I[a,b]	0.464	0.199	0.419	0.827	0.119	0.144
APP V717I[b]	0.480	0.203	0.426	1.107	0.137	0.124
PSEN1 Y115H[b]	1.180	0.277	0.247	2.624	0.163	0.060
PSEN1 M139V[a,b]	0.918	0.223	0.225	3.733	0.180	0.048
PSEN1 Intron 4[b]	1.175	0.226	0.193	2.407	0.128	0.053
PSEN1 R278I[b]	0.504	0.130	0.236	1.131	0.079	0.070
PSEN1 E280G[a]	1.867	0.126	0.076	1.806	0.100	0.055
PSEN1 E280G	1.034	0.151	0.146	2.338	0.113	0.048

Gene	Mutation	Number of individuals
APP	p.Thr719Asn	1 AR
	p.Val717Gly	2 S
	p.Val717Ile	1 S, 7 AR
	p.Val717Leu	2 S, 2 AR
PS1	Intron 4	2 S, 5 AR
	p.Ala79Val	1 S
	p.Tyr115His	1 S, 1 AR
	p.Glu120Lys	1 AR
	p.Ser132Ala	2 AR
	p.Met139Val	1 S, 1 AR
	p.Val142Ile	1 S
	p.Met146Ile	2 AR
	p.Glu184Asp	2 S, 4 AR
	p.Ile202Phe	4 AR
	p.Gly206Ala	1 S
	p.His214Tyr	3 AR
	p.Ala246Glu	2 AR
	p.Pro264Leu	2 AR
	p.Pro267Ser	1 S
	p.Arg269His	1 AR
	p.Arg278Ile	3 AR,
	p.Glu280Gly	2 S, 6 AR,
	ΔE9*	1 S